

GWSkyNet-Multi II: an updated deep learning model for rapid classification of gravitational-wave events

NAYYER RAZA ^{1,2} MAN LEONG CHAN ³ DARYL HAGGARD ^{1,2} ASHISH MAHABAL ^{4,5} JESS MCIVER ³
AUDREY DURAND ^{6,7} ALEXANDRE LAROUCHE ⁶ AND HADI MOAZEN ⁶

¹*Department of Physics, McGill University, 3600 rue University, Montréal, QC H3A2T8, Canada*

²*Trottier Space Institute at McGill, 3550 rue University, Montréal, QC H3A2A7, Canada*

³*Department of Physics and Astronomy, University of British Columbia, Vancouver, BC V6T1Z1, Canada*

⁴*Division of Physics, Mathematics and Astronomy, California Institute of Technology, Pasadena, CA 91125, USA*

⁵*Center for Data Driven Discovery, California Institute of Technology, Pasadena, CA 91125, USA*

⁶*Department of Computer Science and Software Engineering, Université Laval, Québec, QC G1V0A6, Canada*

⁷*Canada CIFAR AI Chair, Mila, Montréal, QC H2S3H1, Canada*

ABSTRACT

Multi-messenger observations of gravitational waves and electromagnetic emission from compact object mergers offer unique insights into the structure of neutron stars, the formation of heavy elements, and the expansion rate of the Universe. With the LIGO-Virgo-KAGRA (LVK) gravitational-wave detectors currently in their fourth observing run (O4), it is an exciting time for detecting these mergers. However, assessing whether to follow up a candidate gravitational-wave event given limited telescope time and resources is challenging; the candidate can be a false alert due to detector glitches, or may not have any detectable electromagnetic counterpart even if it is real. **GWSkyNet-Multi** is a deep learning model developed to facilitate follow-up decisions by providing real-time classification of candidate events, using localization information released in LVK rapid public alerts. Here we introduce **GWSkyNet-Multi II**, an updated model targeted towards providing more robust and informative predictions during O4 and beyond. Specifically, the model now provides normalized probability scores and associated uncertainties for each of the four corresponding source categories released by the LVK: glitch, binary black hole, neutron star-black hole, and binary neutron star. Informed by explainability studies of the original model, the updated model architecture is also significantly simplified, including replacing input images with intuitive summary values, making it more interpretable. For significant O4 event alerts issued between May 2023 and December 2024, **GWSkyNet-Multi II** produces a prediction that is consistent with the updated LVK classification for 93% of events. The updated model can be used by the community to help make time-critical follow-up decisions.

Keywords: Gravitational wave astronomy (675) — Gravitational wave sources (677) — Neural networks (1933)

1. INTRODUCTION

The LIGO-Virgo-KAGRA (LVK) gravitational-wave (GW) observatories (Acerese et al. 2015; Aasi et al. 2015; Akutsu et al. 2021) have reported 90 significant events involving the merger of binary black holes (BBH), neutron stars and black holes (NSBH), and binary neutron stars (BNS) in published event catalogs across their

first three observing runs (Abbott et al. 2019, 2023a, 2024). With the fourth LVK observing run (O4) currently underway, candidate merger events are being detected regularly (~ 200 significant candidates between May 2023 and December 2024), the most promising of which are disseminated by the LVK collaboration in rapid open public alerts¹. This enables follow-up telescope observations of the candidate merger events to

Corresponding author: Nayyer Raza
nayyer.raza@mail.mcgill.ca

¹ <https://gracedb.ligo.org/superevents/public/O4/>

capture any electromagnetic (EM) counterpart emission from the GW source².

Merger events that involve a neutron star (NS) are prime candidates for having associated EM bright emission, as was observed for the BNS merger GW170817 (Abbott et al. 2017a), and the subsequent kilonova AT2017gfo (Abbott et al. 2017b) and short gamma-ray burst GRB 170817A (Abbott et al. 2017c). Multimessenger events are scientifically rich and offer vast discovery potential, giving insights into varied phenomena such as heavy element nucleosynthesis, neutron star structure, and the expansion rate of the universe (Abbott et al. 2017d) (see, e.g., Branchesi et al. (2021) for a review of EM counterparts to GW sources). With a single event offering such a wealth of information, other follow-up detections will enable more robust scientific investigations of these types of mergers.

However, telescope time and resources for follow-up are limited, and require careful consideration of the candidate event. Terrestrial sources and chance noise fluctuations can mimic real astrophysical merger events in the LVK detectors (Abbott et al. 2018, 2020), impact the source parameter estimation when in the vicinity of astrophysical signals (e.g., Dal Canton et al. 2014; Pankow et al. 2018; Powell 2018; Hourihane et al. 2022; Macas et al. 2022; Payne et al. 2022; Ghonge et al. 2024; Udall et al. 2024), and lead to the release of false alarms. Indeed, in the third observing O3, there were 77 rapid public alerts issued for compact binary coalescence (CBC) events³, but subsequent detailed analysis determined only 43 of these (56%) were confidently astrophysical in nature (i.e., included in the GWTC-2.1 and GWTC-3 catalogs). Follow-up observations of false alerts can waste precious telescope resources and time.

Even for the astrophysical events, the potential for having a detectable EM counterpart depends on the type of merger. BNS mergers are the most promising, and are known to produce short gamma-ray bursts and kilonovae, as was observed with GW170817. NSBH mergers may produce an electromagnetic signal (kilonova, GRB) if the NS is tidally disrupted by the black hole (BH) before merger, the probability of which is determined by the mass ratio of the two objects, the aligned spin components, and the NS equation of state (e.g., Barbieri et al. 2020). To-date no EM counterpart to an NSBH merger has been detected (e.g., Vieira et al. (2020)). On the other hand, BBH mergers in the stellar mass range are not typically expected to produce any counterpart,

due to the absence of baryonic matter in the merger surrounding (see, e.g., Branchesi et al. 2021). For mergers involving neutron stars, the EM counterpart, in particular the kilonova, is also expected to be a transient phenomena that can brighten and fade on the order of hours to weeks across ultraviolet to radio wavelengths, and so the follow-up observations are also time sensitive (see, e.g., the review of kilonovae in Metzger 2019). A fast automated classifier of the candidate LVK events that is open to the public can thus serve as a powerful complementary tool to help make time-critical follow-up decisions.

GWSkyNet (Cabero et al. 2020) is a convolutional neural network (CNN) based glitch-vs-real classifier developed for O3 events, which has been further refined and updated by Chan et al. (2024) for O4 events and implemented in the LVK low-latency alert pipeline. The glitch-vs-real model was expanded upon in **GWSkyNet-Multi** (Abbott et al. 2022) as a series of three one-vs-all classifiers to further classify the real (astrophysical) sources as BBH or mergers involving NS (BNS+NSBH). In all iterations the models use low-latency sky map information and associated metadata generated by the rapid localization pipeline **BAYESTAR** (Singer & Price 2016), with the CNN implemented to extract its own features from the localization images. The classifiers have been shown to perform well on O3 alerts, and are currently being used to make predictions for O4 event alerts⁴ (Chan et al. 2024).

In this work we update the **GWSkyNet-Multi** classifier for O4 events, motivated by the findings in Raza et al. (2024) which explained the model’s predictions and identified its limitations and biases. In particular, this included the learned model bias for associating events involving the Virgo detector with astrophysical sources (as compared to glitches), having a discrepancy for annotating the input detector network (online vs triggered), and being insensitive to the signal-to-noise factor of the event. We aim to modify or remove the inputs to the model that do not contribute to the predictions, and wholly update the training dataset to include a more representative sample of LVK events. Additionally, we significantly simplify the model architecture, while making the predictions more informative and nuanced by providing normalized probability scores and uncertainties for the four classes: glitch, BBH, NSBH, and BNS. These updates make predictions for events occurring in LVK O4 and beyond more accurate and robust to the type of event.

² <https://emfollow.docs.ligo.org/userguide/>

³ <https://gracedb.ligo.org/superevents/public/O3/>

⁴ <https://nayyer-raza.github.io/projects/GWSkyNet-Multi/>

The organization of the paper is as follows. In Section 2 we describe the updates made to the model architecture, the training data, and the general model training procedure. In Section 3 we evaluate the model’s performance on test set data and O3 alerts, analyzing the misclassified and high interest events, and make predictions for O4 alerts. In the final section we summarize and offer concluding remarks.

2. MODEL UPDATES

2.1. Updates to architecture

We make significant changes to the architecture of `GWSkyNet-Multi` in our effort to make the model simpler and the inputs more interpretable while still maintaining the model’s performance. Motivated by our findings in Raza et al. (2024), in the current study we experimented with modifying each input and each branch of the `GWSkyNet-Multi` model to study its impact on the model’s performance, and to find the best representations of the data that made the classifications possible. Here we describe the changes made to arrive at the final model, which we call `GWSkyNet-Multi II`.

For the model inputs we remove the sky localization images and the 3D volume projection images (along with their pixel normalization inputs). The original `GWSkyNet-Multi` models were developed with these images given as inputs with the expectation that the convolutional branches in the model would extract useful features from them. In updating the model with the aim to make the inputs more interpretable, we replace each of the images with a representative numerical value that is more physically intuitive. For the sky map image this corresponds to the 90% credible interval of the sky localization area (in deg^2), since we found in Raza et al. (2024) that the model was focusing on the size of the localization region in the sky map images to distinguish between astrophysical and glitch events. The sky area represents how well localized the source is on the sky for follow-up observations with telescopes. For the volume projection images we use the 90% credible interval of the 3D volume localization (in Mpc^3), as this value is related to the sky localization area but also takes into account the distance, and thus indicates the survey volume that would need to be investigated in follow-up observations. Adding values for other credible interval percentages (for example the 50% localization area or volume) does not increase the performance of the models.

For the distance inputs we replace the maximum distance with the standard deviation of the distance (which was previously used to calculate the maximum distance), as a direct measure of the localization uncertainty. Thus the volume (3D), sky area (2D), and distance uncer-

tainty (1D) values offer different representations of the common underlying localization that `BAYESTAR` computes.

Finally, we re-normalize the Bayes signal vs noise ratio (Log BSN) so that it is clipped at a maximum value of 100; events with Log BSN values of > 100 are thus replaced with the value $\text{Log BSN} = 100$. While we found in Raza et al. (2024) that the Log BSN factor was not contributing to the model outputs, after clipping the extreme values we find that it can be a useful discriminant between astrophysical events and glitches.

With a sizable reduction in the complexity of the input parameters, we are also able to significantly reduce the complexity of the model architecture. The final `GWSkyNet-Multi II` model, shown in Figure 1, is a single multi-class classifier (as opposed to three one-vs-all classifiers in `GWSkyNet-Multi`) and has only three layers following the concatenated inputs: 1) a dense layer of 8 neurons, 2) a second dense layer of 8 neurons, and 3) the final output dense layer of 4 neurons, each of which outputs the probability of the event belonging to one of the four classes: Glitch, BBH, NSBH, and BNS. The total number of trainable parameters in the updated multi-class model architecture is 188, compared to a total of 11058 parameters across the 3 one-vs-all models in `GWSkyNet-Multi`. This represents a factor of ~ 60 reduction in the complexity of the model, without compromising the model performance. The change not only allows a significantly shorter training time (allowing us to explore a wider hyper-parameter space for the same compute time), but also results in a model that is potentially easier to study with explainability tools that can give us insights into the features learned.

We emphasize that the updated model now annotates an additional class label, arising from splitting the NS branch into NSBH and BNS, and provides more information to the end user. By using a *softmax* activation function in the final layer we also get normalized prediction probabilities for each of the class types, which can then be directly compared to each other. The updated model thus provides a more complete breakdown of classifications, and also allows for a direct comparison to the preliminary LVK alert classifications.

2.2. Updates to dataset

The training dataset for glitch events has been updated to now only include events from the LVK third observing run O3 (compared to O1+O2 for `GWSkyNet-Multi` as in Abbott et al. (2022)). These events are selected from the trigger list of significant and sub-threshold events that were identified in the final offline analysis of the O3 data with a false alarm

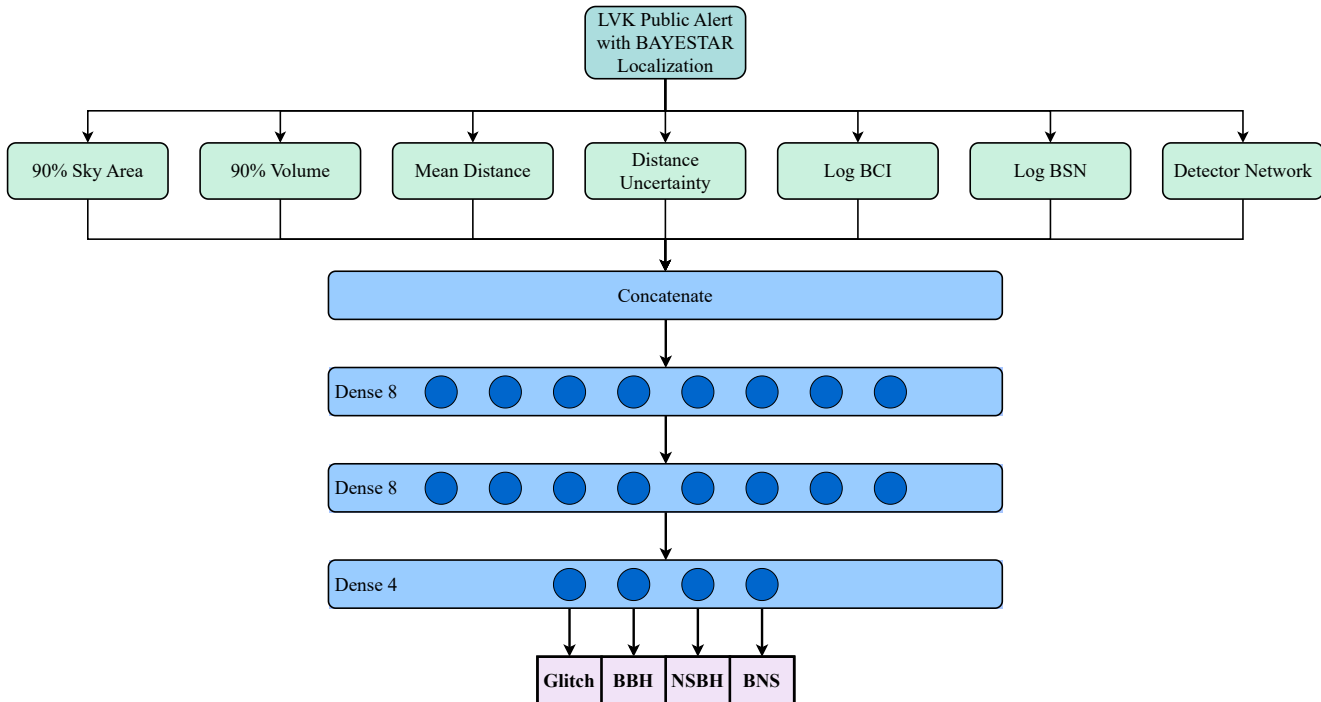


Figure 1. The updated model architecture for `GWSkyNet-Multi II`, showing the flow of information from the LVK public alert to the final classification by the model. Each input corresponds to a single numerical value, except for the detector network which is a vector of 3 binary (0 or 1) values, representing the observing state of the three detectors. The total 9 inputs are concatenated and fully connected to subsequent dense layers. The dense layers use a *ReLU* (rectified linear unit) activation function, while the final layer uses a *softmax* activation function and outputs four classification probabilities, corresponding to the source being a glitch, BBH, NSBH, or BNS. The total number of trainable parameters in the updated model is 188, compared to a total of 11058 parameters in `GWSkyNet-Multi`, representing a factor of ~ 60 reduction in the complexity of the model. This results in a significantly shorter training time and a model that is easier to study with explainability tools.

rate $\text{FAR} < 2/\text{day}$ (Abbott et al. 2021a,b), as outlined in Abbott et al. (2023a). There are a total of 1971 unique events identified in the final O3 catalog (O3a+O3b) across three different modeled matched-filter search pipelines for CBC events: GSTLAL (Cannon et al. 2021), PyCBC (Davies et al. 2020), and MBTA (Aubin et al. 2021). For events that are identified by more than one pipeline, we follow the same procedure as the LVK low-latency analysis⁵ in selecting the preferred pipeline event; 3-detector triggers are given preference over 2-detector triggers, and among those, higher signal-to-noise ratio (SNR) events are given preference over lower SNR events. Of the 1971 unique events in O3, we consider a sub-selection based on the following criteria: (i) the estimated probability of astrophysical origin $p_{\text{astro}} < 0.5$, (ii) the pipeline found a trigger in at least two detectors with single detector SNR $\rho_{\text{det}} > 4.0$, and (iii) the combined network SNR of the event $\rho_{\text{net}} > 6.5$.

⁵ <https://emfollow.docs.ligo.org/userguide/analysis/superevents.html>

A total of 1868 unique events (95%) pass these criteria and are included in our final dataset as glitch events.

There is a possibility that some of the 1868 events that we annotate as glitches are in fact weak astrophysical signals, and thus there is some contamination in our glitch training data. However, this number is expected to be low: for the sub-threshold candidate events (which make up almost all of our glitch dataset) it is estimated that $\lesssim 1\%$ of events are astrophysical (Abbott et al. 2023a). We consider this contamination rate to be low enough as to not have any significant impact on the model training or how it might learn to differentiate between glitches and astrophysical events. As the LVK detectors undergo upgrades between each run, the sensitivity of the detectors and their noise profile naturally also change, which means that we do not fully capture all of the new kinds of transient glitch events that could occur in O4. Nevertheless, by using the latest publicly available datasets, the 1868 glitches from O3 in our updated training data are more representative of the instrumental artifacts expected in O4, as compared to using glitches from O1 and O2.

The astrophysical events (BBH, NSBH, BNS) are simulated events that are injected into Gaussian noise colored by the power spectral densities (PSDs) of the detectors during O3. We generate 1868 simulated events for each of the three astrophysical event types, with the number of events chosen to match the number of glitch events in the training dataset. The simulated events in the updated dataset largely reflect updates to population model fit parameters compared to those available when `GWSkyNet-Multi` was first developed (Abbott et al. 2022). The BH masses are sampled from a power law + peak model with parameters determined from the population in GWTC-3 (Abbott et al. 2023b). For NS masses we follow the distribution determined in Landry & Read (2021) from the population of GW merger events with NS, and sample the masses uniformly in the range $[1 M_{\odot}, 2.5 M_{\odot}]$ with random pairing (the maximum NS mass of $2.5 M_{\odot}$ is chosen as a compromise between the two different values determined in Landry & Read (2021), depending on the exclusion or inclusion of the event GW190814 in the model fits: $m_{max} = 2.0^{+0.4}_{-0.3}$ and $m_{max} = 2.7^{+0.2}_{-0.2}$). For BBH events we constrain the mass ratio according to the distribution in Abbott et al. (2023b), and for NSBH events the mass ratio is constrained to be $q = m_1/m_2 \leq 30$, determined by the 99% confidence interval upper limit of the mass ratio for NSBH events from binary evolution simulations in Drozda et al. (2022). For the spins we assume a simple uniform distribution with aligned spins in the range $[0, 0.99]$ for BHs and $[0, 0.05]$ for NSs. The distances for events are sampled uniformly in volume, and the remaining extrinsic source parameter angles (longitude, latitude, inclination, polarization) are sampled uniformly.

To simulate the astrophysical event waveforms we use the `TaylorF2` (Mishra et al. 2016) waveform model for events with $m_1 + m_2 < 4 M_{\odot}$, and the `SEOBNRv4-ROM` (Bohé et al. 2017) models otherwise. Each waveform is then injected into Gaussian noise colored by the actual PSD of the Hanford, Livingston, and Virgo detectors during one of the confident astrophysical events in O3. We randomly sample from ~ 40 such distinct O3 event PSDs, as provided in the GWTC-2.1 and GWTC-3 data releases (Abbott et al. 2021a,b). The events are distributed such that the number of events simulated in each detector combination (HLV, HL, HV, or LV) is equal. With the $1868 \times 3 = 5604$ simulated astrophysical events, the model can learn the distinguishing features of the underlying sources more robustly.

Based on biases identified in Raza et al. (2024) for the type of events included in training the model, we also lower the SNR threshold for events, and modify the detector status input to be in line with the LVK low-

latency annotation. In `GWSkyNet-Multi` the threshold for including events was set so that the matched filter SNR in at least two detectors was $\rho_{det} > 4.5$, and the network SNR $\rho_{net} > 7$. Since events with lower SNR can be part of public alerts, we lower this threshold so that in our updated dataset we have events with $\rho_{det} > 4.0$ and $\rho_{net} > 6.5$. In `GWSkyNet-Multi` the detector status was based on which detectors had a trigger identified by one of the pipelines. For the glitches, the detector network status is updated to reflect whether or not each individual detector (Hanford, Livingston, or Virgo) was in observing mode at the time of the event, and thus contributed to the sky-localization, regardless of whether one of the pipelines found a corresponding trigger in the detector or not. For example, if an event occurred while all three detectors were in observing mode, but there was a trigger found in only the Hanford and Livingston detectors and not Virgo, this would now be annotated as a three-detector HLV event rather than a 2-detector HL event. Similarly, for the astrophysical events in our dataset, the detector network status corresponds to the detector combination in which we simulate injecting waveforms and use to construct the sky localization, regardless of whether the resulting waveform SNR in each of the detectors would be high enough to trigger a detection pipeline. The detectors that contributed to the sky localization (as opposed to the detectors for which a trigger was found) is part of the information that is made publicly available by the LVK in its alerts, and so the updated data set now replicates the actual alert contents for O4 more closely.

The resulting distributions of key inputs for the glitch, BBH, NSBH, and BNS events are shown in Figure 2. The glitch events have distinct features compared to the astrophysical events for most inputs, except for the Bayes coherence-vs-incoherence ratio (Log BCI). This is a marked change compared to the Log BCI distributions for the dataset used in `GWSkyNet-Multi` (see Figure 1 in Raza et al. (2024)). The glitches used in the previous dataset had lower Log BCI values, possibly arising from the fact that there was no FAR threshold cutoff used to decide which glitch events to include. Among the astrophysical events, we can see that the mean distance estimate and 90% credible volume can distinguish between the three merger classes. We thus expect the models to exploit these differences to learn the correct classifications.

As can be seen in Figure 2, some of the input parameters can span several orders of magnitude for the range of events we consider in our dataset. To avoid numerical issues during model training, we pre-process the data by transforming and normalizing the input values:

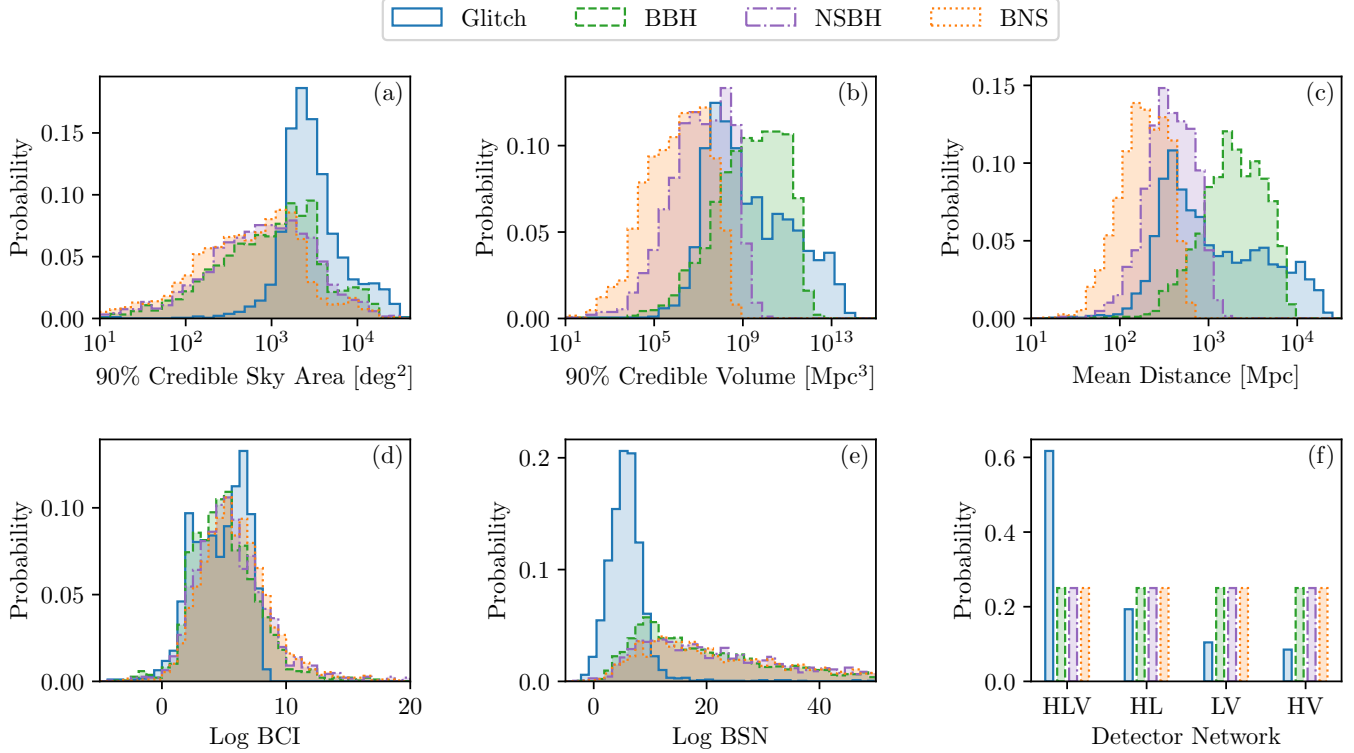


Figure 2. Probability distributions of the updated input parameters to `GWSkyNet-Multi II` over the entire data set of events for the glitch (blue solid line), BBH (green dashed line), NSBH (purple dash-dotted line), and BNS (orange dotted line) sources: (a) sky map localization area, (b) 3D volume localization, (c) estimated mean distance to the source, (d) Bayes factor for coherence versus incoherence, (e) Bayes factor for signal versus noise, and (f) the network of detectors observing during the event. The distributions are distinct for certain input types and thus we expect that the models will learn to use these features to discriminate between source classes. In particular, the sky map localization area and Log BSN factors can potentially distinguish between glitch events and astrophysical sources. While the mean distance estimate and 90% credible volume could be leveraged to classify between BBH, NSBH, and BNS mergers.

i) for the sky area, volume, and distances we first take the logarithm of the values, and ii) for all inputs we then normalize the values by dividing them by the maximum value in the dataset.

2.3. Model training and uncertainty estimation

We randomly split the 7472 events in our final dataset into three categories: i) 81% of events are used for training the model, ii) 9% of events are used for validation during training, and iii) 10% are a hold-out reserved for testing the model’s performance after the training has completed. `GWSkyNet-Multi II` is developed and trained using `TensorFlow` (Abadi et al. 2015) and `Keras` (Chollet et al. 2015). We use the `Adam` optimization algorithm (Kingma & Ba 2014) with a learning rate of 0.001 and a batch size of 64 to train the model, setting the categorical cross-entropy loss as our objective function to minimize. The maximum number of training epochs allowed is 2000. The performance of the model is evaluated after each training epoch by calculating the cross-entropy loss of the validation set, and the train-

ing is stopped early if the validation loss does not decrease for 100 consecutive epochs. This early-stopping based on the validation set performance ensures that the model does not over-fit to the training data. To ensure that the final model is a result of the model learning features from the training set and reaching a global minimum loss, rather than a serendipitous case of initializing with the best weights, we repeat the training five times with different random weight initializations each time. From these five trained models we select the one which has the median accuracy on the validation set (as the representative case, and find only a marginal accuracy difference of $\sim 1 - 2\%$ between the highest and median performing models). The training hyperparameter values for the learning rate, batch size, maximum number of epochs, and patience of early-stopping are manually tuned and the final values chosen such that the model’s performance on the validation set is optimized (maximum accuracy). During training, we also down-weight the BNS and NSBH events by a factor of 10 and 5, respectively, as we find this helps the models generalize

better to events in O3. This is discussed in more detail in Appendix A.

A single trained model outputs four probability values, but does not give any indication of the uncertainties associated with each probability, which would be a useful measure of the model’s confidence in the predictions. In our training we split our dataset so that 90% of the dataset is used for training and validation, while the remaining 10% is kept for testing the model after training, with the events randomly shuffled before doing the split. To compute the uncertainty in the model’s predictions, we generate 20 randomized train-test splittings of the dataset, and train 20 separate models, one for each randomized split. To compute the predictions for each event, the output probabilities from all 20 models are combined and the probability mean and standard deviation for each class is calculated and reported as the final value. Thus we use an ensemble of 20 models trained on slightly different data to determine the uncertainty on the predictions. When a single classification label is required for an event (for example, to calculate the accuracy of the model) we select the class which has the highest predicted mean probability (a winner-take-all approach).

2.4. Comparison to alternate models

Since the updated model inputs are all numerical values (tabular data), we are not constrained to the neural network model architecture (which is known to perform well for image-based inputs), but can also explore alternate supervised learning models that are known to perform well on numerical (tabular) input data. We train two such state-of-the-art models: i) eXtreme Gradient Boosting (XGBoost, [Chen & Guestrin 2016](#)), which implements gradient boosted trees, and ii) Explainable Boosting Machine (EBM, [Lou et al. 2013](#); [Nori et al. 2019](#)), which is a tree-based gradient boosting generalized additive model, and has the advantage of being fully interpretable. We train the XGBoost and EBM models with the same inputs as the neural network, and use `Optuna` ([Akiba et al. 2019](#)), an automatic hyperparameter optimization framework, to select the best model hyperparameters over 5000 trials.

Table 1 shows the classification performance of XGBoost and EBM, as compared to the neural network, for the final selected models. The results show that while XGBoost and EBM have similar accuracy as the neural network on the test set of events, they perform considerably worse on the O3 events (by $\sim 10 - 15\%$). The features learned by the XGBoost and EBM models on the training data thus do not generalize as well to the O3 event alerts, whereas the neural network has learned

Model	Test Accuracy (%)	O3 Accuracy (%)
NeuralNet	85.1 ± 1.3	81.3
XGBoost	85.6 ± 1.0	66.7
EBM	82.2 ± 1.4	72.0

Table 1. A comparison of the classification accuracy scores of three different state-of-the-art machine learning models: Neural Network (NeuralNet), eXtreme Gradient Boosting (XGBoost), and Explainable Boosting Machine (EBM). We compare the prediction accuracy for two datasets: the hold-out test set of events which has the same underlying distribution as the training data, and the O3 event alerts which correspond to the events that were released by the LVK during the third observing run (see Section 3 for more details). The NeuralNet, XGBoost, and EBM models have comparable accuracy for events in the test set, but NeuralNet significantly outperforms XGBoost and EBM for O3 events. We thus select the neural network model as our chosen model and architecture for `GWSkyNet-Multi II`.

more generalized features that transfer well across the two different data sets. We thus proceed with the neural network as our preferred model for `GWSkyNet-Multi II`.

3. PREDICTIONS AND ANALYSIS

We evaluate the predictions of the updated model, `GWSkyNet-Multi II`, on three distinct sets of events: i) the 10% of events from our dataset that were kept as a hold-out test set, ii) the 75 multi-detector public alerts issued by the LVK during O3, and iii) the 180 significant multi-detector public alerts issued by the LVK in the current O4 run, up to the end of December 2024.

3.1. Performance on Test Set Events

The accuracy of the multi-class model predictions for the hold-out test set along with a comparison to previous iterations of the model is shown in Figure 3. For the multi-class model the predicted class label is determined by the class with the highest probability score from the four values. The final `GWSkyNet-Multi II` model, denoted as the multi-class model in the figure, has an accuracy of 85% on the hold-out test set which contains 747 events equally distributed between the four classes of glitch, BBH, NSBH, and BNS. The high accuracy shows that the model effectively fits the data, enabling it to differentiate between all four classes. This is also apparent if we evaluate the model’s performance by aggregating the multi-class predictions for 3 out of the 4 classes and considering it as a binary one-vs-all classifier for each combination: Glitch-vs-all, BBH-vs-all, NSBH-vs-all, and BNS-vs-all (i.e., comparing probability $p(class)$ to $p(not\ class)$ and using a threshold of 0.5 for classification). In all four cases the test accuracy

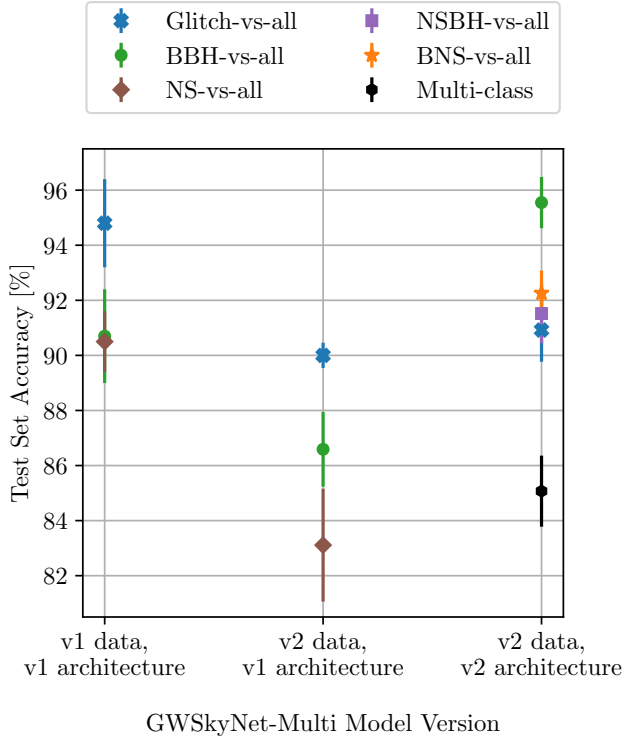


Figure 3. Model performance changes as the dataset and architecture are updated, characterized by the test set accuracy. Scores in the left-hand column (v1 data, v1 architecture) are for the original `GWSkyNet-Multi` model as described in [Abbott et al. \(2022\)](#). Scores in the right-hand column are for the updated model `GWSkyNet-Multi II` presented in this work (v2 data, v2 architecture), showing both the full multi-class accuracy and the aggregated one-vs-all accuracy scores for easier comparison. Scores in the center represent the intermediate model which has the same architecture as the original model but has been trained on the updated dataset (v2 data, v1 architecture). Upgrades made to the dataset only lead to generally worse performance for the model, indicating that the v2 dataset is inherently harder to distinguish. Subsequent architecture changes bring the performance back to $\sim 90 - 95\%$ accuracy when we compare the aggregated one-vs-all models, with a multi-class accuracy of $\sim 85\%$.

is in the $\sim 90 - 95\%$ range, confirming that the model is generalizing equally well across classes (within small variations of a few percent).

The one-vs-all aggregation also allows us to compare the model’s accuracy explicitly with previous versions of the model, which used a series of three one-vs-all classifiers trained separately: `Glitch-vs-all`, `BBH-vs-all`, and `NS-vs-all`. For each model version the test accuracy is evaluated on a 10% hold-out set of events drawn from the same distribution as its training data. For the previous one-vs-all model versions, the classification threshold was set so that the test set false negative rate and false positive rate were equal (see Figure

4 in [Abbott et al. \(2022\)](#). The comparisons in Figure 3 show that when only the dataset is updated (as described in Section 2.2) while keeping the architecture the same as the original `GWSkyNet-Multi` model ([Abbott et al. 2022](#)), the test accuracy across all three binary classifiers decreases on the order of $\sim 5 - 10\%$. This is likely due to the fact that in the updated dataset the SNR threshold of events is lower, and so includes more events that are harder to distinguish from background noise and thus may have fewer distinct features that the model can learn. Furthermore, the updated dataset for glitch events has a FAR cutoff of 2/day and so does not include some of the loudest and most obvious of glitch events, whereas there was no FAR threshold used in training `GWSkyNet-Multi`. As discussed in Section 2.2, this change is most apparent in the distribution of the Log BCI input value, with `GWSkyNet-Multi` trained on glitches that generally have smaller Log BCI values as compared to astrophysical events, while `GWSkyNet-Multi II` is trained on glitches and astrophysical events that have very similar distributions of the Log BCI values (see Figure 2(d)).

The updates made to the model architecture for `GWSkyNet-Multi II` increase the test accuracy by a significant amount after the dataset updates have been implemented, such that each of the aggregated one-vs-all models have an accuracy that is either equal to (`Glitch-vs-all`) or higher than (`BBH-vs-all`, `NSBH-vs-all`, `BNS-vs-all`) the corresponding model with dataset updates only, demonstrating that the architecture changes contribute positively to the model’s predictive power. While the percentage difference values are not large when comparing the test accuracy of `GWSkyNet-Multi II` to `GWSkyNet-Multi`, the accuracies are all above 90%, showing that it is still in a high performance regime, with small trade-offs in optimizing astrophysical event predictions compared to glitches. Keeping in mind that the updated dataset is inherently harder to distinguish, while the updated model architecture is significantly simpler and provides more predictive information (distinguishes between NS events), `GWSkyNet-Multi II` represents a significant update to the original model.

3.2. Predictions for O3 Public Alerts

There were 77 low-latency public alerts for candidate CBC events issued by the LVK in O3. Of these, two events, S190910h and S190930t, were single detector (Livingston) events. Since `GWSkyNet-Multi II` is trained to predict on multi-detector events, we evaluate the model’s performance on the 75 multi-detector O3 events only. The predictions are made using the

low-latency localization maps that were generated by BAYESTAR and released in the O3 public alerts, as available on GraceDB ⁶. The prediction results from GWSkyNet-Multi II are compared to the true classifications as determined in the full offline analysis of these events by the LVK and published in the final O3 catalogs GWTC-2.1 and GWTC-3 (Abbott et al. 2023a, 2024) (hereafter collectively referred to as GWTC-3 for simplicity). For our analysis, only confident events determined with $p_{\text{astro}} > 0.5$ and included in GWTC-3 are considered astrophysical events, with the rest classified as glitches. Of the astrophysical events, the merger type is determined from each of the best-fit component masses of the binary: if the mass is $< 3 M_{\odot}$ then the component is determined to be an NS; otherwise it is a BH. Thus of the 75 O3 public alerts analyzed, we determine from GWTC-3 that 32 are glitches (which includes 22 alerts that were subsequently retracted by the LVK), 40 are BBH, 2 are NSBH, and 1 is a BNS merger.

A comparison of the GWSkyNet-Multi II predicted classification to the true GWTC-3 classification is shown in Figure 4. Overall, GWSkyNet-Multi II correctly predicts 61/75 (81%) of O3 events. If we only consider the model accuracy for determining glitch-vs-real, i.e., aggregate the astrophysical source classes, then it is able to correctly predict 67/75 (89%) of O3 events.

We note that the off-diagonal values are all zero for the lower half of the confusion matrix, and the misclassifications are concentrated in the upper half of off-diagonal elements. As the classifications shown in Figure 4 are ordered from lowest EM counterpart potential and follow-up priority (glitch) to highest (BNS), this indicates that for O3 events GWSkyNet-Multi II does not produce false negative predictions for promising events, and tends to be conservative in making predictions for an event that would lower its potential for follow-up (i.e., false positives for high potential events are preferred over false negatives). For example, for true NSBH events, GWSkyNet-Multi II only predicts them to be an NSBH or a higher priority BNS event. Conversely, if there is a public alert for a potential NSBH event, but it is actually a glitch, then GWSkyNet-Multi II predicts it to be a glitch only when it is confident that it is not an NSBH or BNS. These results are currently only indicative of any underlying trends the model has learned, as the total number of NSBH and BNS events in O3 is too low for any robust conclusions. A full analysis of the final O4 results will help affirm (or deviate from) these trends.

⁶ <https://gracedb.ligo.org/superevents/public/O3/>

O3 Public Alerts

		24 (0.75)	0 (0.00)	2 (0.06)	6 (0.19)
GWTC-3 True Class	Glitch	0 (0.00)	35 (0.88)	5 (0.12)	0 (0.00)
	BBH	0 (0.00)	0 (0.00)	1 (0.50)	1 (0.50)
	NSBH	0 (0.00)	0 (0.00)	0 (0.00)	1 (1.00)
	BNS	0 (0.00)	0 (0.00)	0 (0.00)	0 (0.00)
	GWTC-3 True Class	Glitch	BBH	NSBH	BNS
		GWSkyNet-Multi II Predicted Class			

Figure 4. Predicted versus true classification confusion matrix for GWSkyNet-Multi II on O3 public alerts. GWSkyNet-Multi II correctly predicts 61/75 (81%) events, with most misclassifications being glitches identified as BNS (6 events), and BBH identified as NSBH (5 events). Crucially, the model does not produce false negative predictions for more promising events, indicating that for O3 alerts it is conservative in “demoting” an event that has a higher potential of having an electromagnetic counterpart to an event class with lower potential.

3.2.1. Analysis of Misclassified Events

A detailed comparison of O3 events misclassified by either GWSkyNet-Multi or GWSkyNet-Multi II is shown in Table 2. Both models have a comparable predictive accuracy, with GWSkyNet-Multi correctly predicting 60/75 (80%) events and GWSkyNet-Multi II correctly predicting 61/75 (81%) events. There are 9 events that were misclassified by GWSkyNet-Multi but are correctly classified by GWSkyNet-Multi II. This crucially includes the BNS merger event S190425z (discussed in detail in the next subsection). 6 events are misclassified by both models; these are predicted to be NS events by GWSkyNet-Multi and BNS or NSBH events by GWSkyNet-Multi II. And finally there are 8 events that were correctly classified by GWSkyNet-Multi but are now misclassified by GWSkyNet-Multi II. These are all glitch or BBH events that are misclassified as NSBH or BNS events, as well as one NSBH event that is misclassified as BNS (S200115j, discussed in detail in the next subsection). With the NS branch split into the BNS and NSBH branches, it becomes clear that the 5 BBH events

that are being misclassified by `GWSkyNet-Multi II` are all predicted to be NSBH. If we compare the mean distance input of these misclassifications, as shown in Figure 6 in Appendix B, we find that all 5 of these misclassified BBH events lie at the lower end of the BBH distribution.

The most dominant misclassifications are of glitch events that are being predicted as NSBH or BNS events. This is a pattern that is seen both with `GWSkyNet-Multi` and `GWSkyNet-Multi II`. For the former, Raza et al. (2024) found that this arose because many of these glitch events had large Log BCI values and smaller sky localization areas, both of which the model had learned to associate with astrophysical events. However, when we attempt to compare the same inputs for the `GWSkyNet-Multi II` misclassifications, we find no obvious trend (see Appendix B). This suggests that the model does not have a linear dependence on any one input, but has learned to distinguish classes from a non-linear combination of the inputs as codified in the updated neural network architecture. A deeper analysis of the model with machine learning interpretability tools could provide insights into its learned decision boundaries, and will be explored in future work.

The fact that `GWSkyNet-Multi II` misclassifies some of the smaller distance BBH events as NSBH, and some of the glitch events as NSBH or BNS, is not ideal for EM follow-up campaigns. Targeting events that in reality have no (or low) potential for having an EM counterpart would lead to a waste of follow-up resources. However, since BNS and NSBH events are rare and have much higher scientific potential, a classifier that produces more false positives for NS events is a better outcome than one that produces false negatives (i.e, potentially misses high interest sources).

We also dis-aggregate the events and misclassifications according to the detector network type: 6/43 (14%) of the 3-detector HLV events are misclassified, and 8/32 (25%) of the 2-detector events are misclassified. Thus `GWSkyNet-Multi II` misclassifies a larger percentage of 2-detector events as compared to 3-detector events. Within the 2-detector events, the fraction of misclassifications are: 5/19 (26%) HL, 3/11 (27%) LV, and 0/2 (0%) HV, indicating that `GWSkyNet-Multi II` has not learned any particular bias for 2-detector combinations. We contrast these to the misclassifications from `GWSkyNet-Multi`: 5/43 (12%) HLV, 2/19 (11%) HL, 6/11 (55%) LV, and 2/2 (100%) HV, which clearly show a bias for misclassifying 2-detector events involving Virgo. This bias, identified in Raza et al. (2024), is thus resolved in the updated model by including more

glitch events in the training data that involve the Virgo detector.

3.2.2. Analysis of NS Merger Events

Three of the O3 alerts are included in the final GWTC-2.1 and GWTC-3 catalogs as confident astrophysical events that involve an NS: i) S190425z (GW190425) as a BNS, ii) S190814bv (GW190814) as an NSBH, and iii) S200115j (GW200115) as an NSBH. In addition, there is one marginal NSBH candidate S200105ae (GW200105). The event is considered marginal because it does not pass the threshold $p_{\text{astro}} > 0.5$, but it does pass the threshold of $\text{FAR} < 2/\text{yr}$. As these merger events (potentially) involve an NS, they are the most promising events of the O3 public alerts that could have an EM counterpart for follow-up observations. For these four events, we compare the corresponding GWTC-3 class probabilities (as determined by the detection pipeline with the highest SNR, see Table XIII and Table XV in Abbott et al. (2023a)) and the predicted class probabilities by `GWSkyNet-Multi II`, in Table 3. While only 4 events is not enough to draw conclusive statements, the comparisons serve to provide some insight into the model through illustrative examples.

For events S190425z and S190814bv, the probability scores that `GWSkyNet-Multi II` predicts and the source probabilities determined by the detecting pipeline in the GWTC-3 final offline analysis are consistent. S190425z is classified by `GWSkyNet-Multi II` as a BNS with $p_{\text{BNS}} = 66 \pm 22\%$, compared to the GWTC-3 probability $p_{\text{BNS}} = 69\%$ (detection pipelines used in GWTC-3 do not report uncertainties). While the uncertainty in the `GWSkyNet-Multi II` prediction for this event is relatively high, the mean prediction probability is very close to the GWTC-3 value. For S190814bv the `GWSkyNet-Multi II` classification is an NSBH with $p_{\text{NSBH}} = 81 \pm 9\%$, compared to the GWTC-3 probability $p_{\text{NSBH}} = 86\%$. The probability scores for the other three classes for this event also agree. The fact that `GWSkyNet-Multi II` is able to give remarkably similar classification probabilities for these two events based on the preliminary low-latency analysis and localization data only, as compared to the final analysis of the fully calibrated strain data in GWTC-3, illustrates its predictive accuracy and utility as a classifier for making rapid follow-up decisions.

On the other hand, the `GWSkyNet-Multi II` probability of NSBH for S200115j, $p_{\text{NSBH}} = 8 \pm 5\%$, is not consistent with the catalog value of $p_{\text{NSBH}} = 100\%$. To get a sense of why `GWSkyNet-Multi II` is mispre-

Event ID	GWSkyNet-Multi II Prediction (%)					GWSkyNet-Multi	GWTC-3
	Glitch	BBH	NSBH	BNS	Classification	Classification	Classification
<i>S190405ar</i>	98 ± 1	0 ± 0	0 ± 0	2 ± 1	Glitch	<i>NS</i>	Glitch
<i>S190425z</i>	27 ± 24	1 ± 2	6 ± 7	66 ± 22	BNS	<i>Glitch</i>	BNS
<i>S190630aq</i>	2 ± 3	98 ± 3	0 ± 0	0 ± 0	BBH	<i>Glitch</i>	BBH
<i>S191213g</i>	93 ± 8	0 ± 0	0 ± 0	7 ± 8	Glitch	<i>NS</i>	Glitch
<i>S191216ap</i>	2 ± 1	94 ± 3	4 ± 2	0 ± 0	BBH	<i>NS</i>	BBH
<i>S191220af</i>	64 ± 16	0 ± 0	1 ± 1	35 ± 15	Glitch	<i>NS</i>	Glitch
<i>S191225aq</i>	70 ± 27	1 ± 2	2 ± 6	27 ± 25	Glitch	<i>NS</i>	Glitch
<i>S200112r</i>	6 ± 7	94 ± 7	0 ± 0	0 ± 0	BBH	<i>Glitch</i>	BBH
<i>S200302c</i>	1 ± 1	99 ± 1	0 ± 0	0 ± 0	BBH	<i>Glitch</i>	BBH
<i>S190426c</i>	28 ± 11	0 ± 0	4 ± 2	68 ± 11	BNS	<i>NS</i>	Glitch
<i>S190503bf</i>	1 ± 1	1 ± 1	83 ± 11	15 ± 10	NSBH	<i>NS</i>	BBH
<i>S190816i</i>	6 ± 4	0 ± 1	43 ± 11	50 ± 11	BNS	<i>NS</i>	Glitch
<i>S190923y</i>	15 ± 9	0 ± 0	18 ± 11	67 ± 12	BNS	<i>NS</i>	Glitch
<i>S190924h</i>	0 ± 0	2 ± 1	97 ± 2	0 ± 1	NSBH	<i>NS</i>	BBH
<i>S200106au</i>	12 ± 19	0 ± 1	4 ± 4	84 ± 18	BNS	<i>NS</i>	Glitch
<i>S190521g</i>	0 ± 0	13 ± 7	87 ± 7	0 ± 0	NSBH	BBH	BBH
<i>S190602aq</i>	0 ± 0	28 ± 9	71 ± 9	0 ± 0	NSBH	BBH	BBH
<i>S190829u</i>	18 ± 17	1 ± 2	7 ± 6	74 ± 16	BNS	Glitch	Glitch
<i>S190930s</i>	1 ± 0	6 ± 3	94 ± 3	0 ± 0	NSBH	BBH	BBH
<i>S191120aj</i>	1 ± 2	0 ± 0	14 ± 11	85 ± 11	BNS	Glitch	Glitch
<i>S200105ae</i>	3 ± 4	1 ± 2	53 ± 17	44 ± 18	NSBH	Glitch	Glitch
<i>S200108v</i>	4 ± 4	8 ± 9	87 ± 9	1 ± 3	NSBH	Glitch	Glitch
<i>S200115j</i>	1 ± 1	0 ± 0	8 ± 5	90 ± 6	BNS	NS	NSBH

Table 2. A comparison of O3 OPA events misclassified by GWSkyNet-Multi (italicized), GWSkyNet-Multi II (bolded), or both (bolded and italicized). The GWTC-3 classifications are obtained by considering only events with $p_{\text{astro}} > 0.5$ as astrophysical (with the rest classified as glitches). The type of binary for the astrophysical events is determined from the best-fit component masses, assuming a maximum NS mass of $3 M_{\odot}$. The event S200105ae has $p_{\text{astro}} = 0.36$ and so we consider it a glitch, but is reported in GWTC-3 as a *marginal* NSBH candidate since it does pass the FAR threshold of $< 2/\text{yr}$. Note in particular the predictions for event S190425z, which is misclassified by GWSkyNet-Multi as a glitch, but is correctly classified as a BNS by GWSkyNet-Multi II.

Event ID	GWSkyNet-Multi II Probability (%)				GWTC-3 Probability (%)			
	Glitch	BBH	NSBH	BNS	Glitch	BBH	NSBH	BNS
S190425z	27 ± 24	1 ± 2	6 ± 7	66 ± 22	31	0	0	69
S190814bv	0 ± 0	18 ± 9	81 ± 9	0 ± 1	0	14	86	0
S200115j	1 ± 1	0 ± 0	8 ± 5	90 ± 6	0	0	100	0
S200105ae	3 ± 4	1 ± 2	53 ± 17	44 ± 18	64	0	36	0

Table 3. A comparison of the classification probability scores of the three O3 OPA events that are included in the final GWTC-3 catalog as confident merger events involving NS, plus the marginal event S200105ae. GWSkyNet-Multi II correctly classifies the first two events with the classification probabilities consistent with those in the GWTC-3 catalog. However, events S200115j and S200105ae are mis-classified (discussed in more detail in Section 3.2.2).

dicting this event as a BNS we look at the masses of the components as determined in [Abbott et al. \(2023a\)](#): $m_1 = 5.9_{-2.5}^{+2.0} M_\odot$, $m_2 = 1.44_{-0.28}^{+0.85} M_\odot$, with chirp mass $\mathcal{M}_c = 2.43_{-0.07}^{+0.05} M_\odot$. The mass of the primary component is at the lower end of the stellar BH mass range, with a 29% probability that $m_1 < 5 M_\odot$ and lies within the lower BH mass gap ([Abbott et al. 2023a](#)). This implies that the BH in this merger is one of the lightest BHs detected in CBCs, and thus the event characteristics might be similar to some of the high-mass BNS events that **GWSkyNet-Multi II** is trained on. The fact that the masses of the system lie close to the boundary of what the model has learned to distinguish between BNS and NSBH events is what leads **GWSkyNet-Multi II** to mis-predict S200115j as a BNS event with $p_{\text{BNS}} = 90 \pm 6\%$.

For the marginal event S200105ae, **GWSkyNet-Multi II** incorrectly predicts the event to be astrophysical with $p_{\text{glitch}} = 3 \pm 4\%$, compared to the GWTC-3 probability of $p_{\text{glitch}} = 64\%$. However we note that the probabilities of the event being an NSBH merger are closer and marginally overlap within the associated uncertainty: $p_{\text{NSBH}} = 53 \pm 17\%$, compared to the GWTC-3 $p_{\text{NSBH}} = 36\%$. As more NSBH events are detected in future observations and we gain a better understanding of the rate of NSBH events, we will have a clearer picture of whether this event is truly a glitch or a weak NSBH signal that is difficult to distinguish from the noise.

3.3. O4 Public Alerts

The LVK fourth observing run, O4, began in May 2023, with the first half of the run (O4a) concluding in January 2024. During this time only the two LIGO detectors, Hanford and Livingston, were in science observing mode and made GW detections. This was followed by a brief period of maintenance and minor upgrades to the detectors, after which the LIGO detectors turned back on in April 2024, now joined by the Virgo detector, marking the start of O4b, which is expected to run until June 2025. The LVK has continued to release low-latency public alerts to the community throughout O4, dividing the alerts into two categories: i) significant candidate events, which have been detected with a false alarm rate $\text{FAR} < 2/\text{yr}$, and ii) low significance events, which have $\text{FAR} < 2/\text{day}$.

For the significant event alerts, the collaboration also provides follow-up alerts for the events, on a time-scale of hours to days, updating the event classification based

on human vetting and a more refined analysis. If the event is determined to arise from terrestrial sources, the alert is retracted and the event is classified as a glitch. Otherwise, a more detailed source parameter estimation is performed when possible, and an update alert is issued with improved estimates of the alert contents, including the latest predicted LVK classification probabilities. For low significance alerts the LVK does not provide follow-up analysis, and any refined predictions will only become available once the observing run has finished and the collaboration releases its final catalog.

In [Table 4](#) we provide the **GWSkyNet-Multi II** predictions for select significant event alerts that have been issued during O4. A regularly updated list of all O4 event predictions, including low significance events, is made publicly available and maintained by the authors⁷. For events that were found by multiple search pipelines (superevents with multiple associated events), the predictions (and comparisons) shown are for the final preferred events as identified in low-latency by the LVK⁸. There have been 180 multi-detector CBC candidate events that have associated **BAYESTAR** localization maps published between May 2023 and December 2024. Of these, there were 17 events that were subsequently retracted as glitch events, and 1 event (S240422ed) that was not retracted but has an updated classification of being a glitch ([Ligo Scientific Collaboration et al. 2024](#)). Three of the alerts that were not retracted have updated LVK probabilities that are consistent with being classified as NSBH. For the rest of the 159 events, the updated LVK classification is a BBH.

An analysis of the accuracy of **GWSkyNet-Multi II** predictions for the O4 events can be done by comparing the predictions to the latest LVK updated predictions. This is a preliminary analysis because the final classification of events only becomes available when the LVK releases the final catalog of events after the observing run has finished. However, comparing to the latest LVK classification gives us a reasonable comparison metric and a check for prediction validity. In [Figure 5](#) we provide a comparison of the **GWSkyNet-Multi II** predicted class (highest probability class) to the LVK updated prediction class (highest probability class). If the LVK updated class is considered to be the true class, then **GWSkyNet-Multi II** correctly predicts 168/180 events, for an accuracy of 93%. For these same events, the LVK preliminary classifications match the updated classifications for 165/180 events (92% accuracy), and so **GWSkyNet-Multi II** has a comparable accuracy to the LVK preliminary predictions.

⁷ <https://nayyer-raza.github.io/projects/GWSkyNet-Multi/>

Table 4. Predictions for select significant O4 events

Event ID	GWSkyNet-Multi II Prediction (%)					LVK	LVK Updated Prediction (%)				
	Glitch	BBH	NSBH	BNS	Class		Preliminary	Glitch	BBH	NSBH	BNS
S230518h	0 ± 0	1 ± 1	28 ± 8	71 ± 8	BNS	NSBH	10	4	86	0	NSBH
S230524x*	100 ± 0	0 ± 0	0 ± 0	0 ± 0	Glitch	BNS*	100	0	0	0	Glitch [†]
S230622ba*	0 ± 0	2 ± 2	92 ± 6	6 ± 6	NSBH	BBH*	100	0	0	0	Glitch [†]
S230627c	0 ± 1	37 ± 21	63 ± 21	0 ± 0	NSBH	NSBH	3	48	49	0	NSBH
S230630am	19 ± 10	81 ± 10	0 ± 0	0 ± 0	BBH	BBH	2	98	0	0	BBH
S230630bq	2 ± 2	73 ± 8	24 ± 8	0 ± 0	BBH	BBH	3	97	0	0	BBH
S230706ah	12 ± 9	87 ± 9	0 ± 0	0 ± 0	BBH	BBH	3	97	0	0	BBH
S230708t	7 ± 10	77 ± 18	15 ± 19	0 ± 0	BBH	BBH	3	97	0	0	BBH
S230708bi*	7 ± 4	93 ± 4	0 ± 0	0 ± 0	BBH	BBH*	100	0	0	0	Glitch [†]
S230708cf	19 ± 7	81 ± 7	0 ± 0	0 ± 0	BBH	BBH	1	99	0	0	BBH
S230712a*	3 ± 3	31 ± 21	65 ± 21	0 ± 0	NSBH	BBH*	100	0	0	0	Glitch [†]
S230715bw*	80 ± 17	0 ± 1	17 ± 17	2 ± 2	Glitch	NSBH*	100	0	0	0	Glitch [†]
S230723ac	1 ± 1	99 ± 1	1 ± 1	0 ± 0	BBH	BBH	13	87	0	0	BBH
S230731an	0 ± 0	96 ± 2	4 ± 2	0 ± 0	BBH	BBH	0	81	18	0	BBH
S230807f	14 ± 6	86 ± 6	0 ± 0	0 ± 0	BBH	BBH	5	95	0	0	BBH
S230810af*	97 ± 13	0 ± 0	0 ± 0	3 ± 13	Glitch	BNS*	100	0	0	0	Glitch [†]
S230830b*	3 ± 4	0 ± 0	9 ± 5	88 ± 6	BNS	NSBH*	100	0	0	0	Glitch [†]
S230918aq*	100 ± 0	0 ± 0	0 ± 0	0 ± 0	Glitch	BNS*	100	0	0	0	Glitch [†]
S230922q	0 ± 0	79 ± 8	21 ± 8	0 ± 0	BBH	BBH	0	100	0	0	BBH
S231030av*	93 ± 16	0 ± 0	0 ± 1	7 ± 16	Glitch	BNS*	100	0	0	0	Glitch [†]
S231112ag*	20 ± 25	80 ± 25	0 ± 0	0 ± 0	BBH	BBH*	100	0	0	0	Glitch [†]
S231113bw	0 ± 0	98 ± 1	2 ± 1	0 ± 0	BBH	BBH	4	96	0	0	BBH
S231118an	0 ± 0	100 ± 0	0 ± 0	0 ± 0	BBH	BBH	24	74	1	0	BBH
S231119u	19 ± 8	81 ± 8	0 ± 0	0 ± 0	BBH	BBH	5	95	0	0	BBH
S240413p*	0 ± 1	95 ± 4	5 ± 4	0 ± 0	BBH	NSBH*	2	98	0	0	BBH
S240420aw*	53 ± 29	47 ± 29	0 ± 0	0 ± 0	Glitch	BBH*	100	0	0	0	Glitch [†]
S240422ed*	58 ± 17	0 ± 0	1 ± 1	41 ± 16	Glitch	NSBH*	93	0	2	5	Glitch
S240423br*	1 ± 2	99 ± 2	1 ± 1	0 ± 0	BBH	BBH*	100	0	0	0	Glitch [†]
S240426s	2 ± 2	0 ± 0	32 ± 13	65 ± 13	BNS	BBH	2	98	0	0	BBH
S240429an	85 ± 26	1 ± 2	2 ± 6	12 ± 23	Glitch	Glitch	100	0	0	0	Glitch [†]
S240618ah	13 ± 6	87 ± 6	0 ± 0	0 ± 0	BBH	BBH	4	96	0	0	BBH
S240621em	58 ± 14	42 ± 14	0 ± 0	0 ± 0	Glitch	BBH	4	96	0	0	BBH
S240623dg	70 ± 37	0 ± 0	1 ± 2	29 ± 36	Glitch	Glitch	100	0	0	0	Glitch [†]
S240627by	15 ± 9	79 ± 9	6 ± 3	0 ± 0	BBH	BBH	1	99	0	0	BBH
S240825ar	2 ± 2	85 ± 5	12 ± 4	0 ± 0	BBH	BBH	1	97	3	0	BBH
S240830gn	0 ± 0	94 ± 3	6 ± 3	0 ± 0	BBH	BBH	0	89	11	0	BBH
S240910ci	0 ± 0	99 ± 1	1 ± 1	0 ± 0	BBH	BBH	0	69	31	0	BBH
S240915b	0 ± 0	99 ± 1	0 ± 0	0 ± 0	BBH	BBH	0	86	14	0	BBH
§240916ar	31 ± 13	64 ± 12	5 ± 3	0 ± 0	BBH	BBH	1	99	0	0	BBH
S240917cb	37 ± 14	63 ± 14	0 ± 0	0 ± 0	BBH	BBH	4	96	0	0	BBH
S240925n	0 ± 1	49 ± 15	51 ± 15	0 ± 0	NSBH	BBH	0	100	0	0	BBH
§241005bo	99 ± 4	0 ± 0	0 ± 0	1 ± 4	Glitch	Glitch	100	0	0	0	Glitch [†]

⁸ <https://emfollow.docs.ligo.org/userguide/analysis/superevents.html>

S241011k	1 ± 1	89 ± 7	10 ± 7	0 ± 0	BBH	BBH	0	100	0	0	BBH
S241102br	0 ± 1	43 ± 18	57 ± 18	0 ± 0	NSBH	BBH	0	99	1	0	BBH
S241104a	83 ± 9	5 ± 4	13 ± 6	0 ± 0	Glitch	Glitch	100	0	0	0	Glitch [†]
S241109bn	2 ± 1	40 ± 12	58 ± 12	0 ± 0	NSBH	NSBH	0	28	72	0	NSBH
S241110br	4 ± 2	34 ± 12	62 ± 13	0 ± 0	NSBH	BBH	0	100	0	0	BBH
S241114y	2 ± 4	85 ± 7	12 ± 8	0 ± 0	BBH	BBH	0	100	0	0	BBH
S241126dm*	75 ± 37	7 ± 13	16 ± 30	2 ± 7	Glitch	BBH*	100	0	0	0	Glitch [†]
S241130n	3 ± 3	82 ± 6	15 ± 5	0 ± 0	BBH	BBH	0	100	0	0	BBH
S241201ac	24 ± 11	76 ± 11	0 ± 0	0 ± 0	BBH	BBH	3	97	0	0	BBH
S241210cw	23 ± 9	77 ± 9	0 ± 0	0 ± 0	BBH	BBH	0	100	0	0	BBH

Table 4. *GWSkyNet-Multi* II predictions for select significant O4 events. Of the 180 multi-detector CBC candidate events with BAYESTAR maps published between May 2023 and December 2024, we show all events except for those for which both the LVK and *GWSkyNet-Multi* II predicted probabilities of BBH are $> 90\%$ (i.e., we omit events that are confidently predicted as BBH by both classifications). The remaining 52 events are listed here. Events for which the predicted *GWSkyNet-Multi* II class and LVK updated class (on GraceDB) do not match are highlighted in bold (12/180). Events for which the LVK preliminary class and LVK updated class do not match are indicated with an asterisk (*) (15/180). If the LVK updated class is a glitch due to the event alert being retracted by the LVK, the prediction class is annotated with a dagger (†) (17 events). The horizontal line in the middle of the table indicates the boundary between the two halves of the fourth observing run, O4a and O4b. Note in particular the event S240422ed, a high interest potential NSBH alert, which *GWSkyNet-Multi* II predicted to likely be a glitch with a probability of 58%, and the LVK updated the classification after further analysis to be consistent with a glitch as well.

Continuing the comparison to the LVK updated class, the vast majority (97%) of BBH events are correctly identified by *GWSkyNet-Multi* II, and of the 3 NSBH events, one is misclassified as a BNS merger. For the glitch events we see a similar trend as for the O3 predictions; *GWSkyNet-Multi* II correctly predicts most as glitches, but not all are identified as false alarms, with 6/18 (33%) misclassified as astrophysical events. While the overall accuracy of 93% in this initial analysis of the model is promising, we leave a more detailed analysis of the misclassifications to future work, once the final LVK O4 catalog is available and there is more complete information about the true nature of the event sources. The comparison to final classifications will help illuminate the strengths and weaknesses of not only the *GWSkyNet-Multi* II model, but also *GWSkyNet* II (Chan et al. 2024), which is targeted towards and optimized for glitch-vs-real classifications only, with different training data, architecture, inputs, and reported outputs.

4. SUMMARY AND CONCLUSION

In this work we have introduced *GWSkyNet-Multi* II, a real-time deep learning classifier for gravitational-wave events that offers a significant update to the original model for predictions in O4 and beyond.

Motivated by the findings in Raza et al. (2024), we update the training dataset to include examples of glitch events from the LVK O3 run, and simulate astrophysical events from updated population models. The detector network input is modified to more accurately mirror the

information available in the public alerts, which allows us to include examples of glitches that were observed in the 3 detector HLV configuration. The SNR threshold for including events in the data is also reduced, to better capture low significance event alerts that are published by the LVK in O4. This provides a less biased and more representative sample of LVK events to train the model.

The model architecture is significantly simplified while making the predictions more informative. The three one-vs-all models in *GWSkyNet-Multi* (glitch, BBH, NS) are replaced by a single multi-class classifier that gives normalized probability scores for all four CBC candidate event categories released by the LVK: glitch, BBH, NSBH, and BNS. Thus the model is now able to distinguish between NSBH and BNS events. The 2D sky map and 3D volume projection image inputs are replaced by the 90% confidence interval values for the sky area and volume, respectively. This removes the convolutional branch of the model and reduces the inputs to numerical (tabular) data only. The maximum distance is replaced by the distance uncertainty estimate, while the log BSN input is re-normalized to a maximum value of 100.

The architecture is simplified such that it has only 20 neurons in total: two fully connected hidden layers of 8 neurons each followed by an output layer of 4 neurons. This represents a factor of 60 reduction in the number of trainable parameters, as compared to *GWSkyNet-Multi*. By taking an ensemble of predictions, the model also provides uncertainties associated with each classification probability, giving more information to the end user for how confident the model predictions are. The simplicity

O4 Significant Public Alerts

LVK Updated Class	Glitch	12 (0.67)	3 (0.17)	2 (0.11)	1 (0.06)
	BBH	1 (0.01)	154 (0.97)	3 (0.02)	1 (0.01)
	NSBH	0 (0.00)	0 (0.00)	2 (0.67)	1 (0.33)
	BNS	0 (nan)	0 (nan)	0 (nan)	0 (nan)
		GWSkyNet-Multi II Predicted Class			
		Glitch	BBH	NSBH	BNS

Figure 5. Confusion matrix showing GWSkyNet-Multi II predictions for all 180 multi-detector significant CBC events in O4 (published up to the end of December 2024), compared to the LVK latest (updated) classification. This includes 17 events that have been retracted by the LVK as glitches, and the event S240422ed, which has not been retracted but the event classification probability has been updated by the LVK to be likely a glitch (see Table 4). If the LVK updated class is considered to be the true class, then GWSkyNet-Multi II has a prediction accuracy of 93% for O4 significant events.

of the architecture, combined with the more intuitive numerical (tabular) inputs, make GWSkyNet-Multi II a more interpretable model.

The updated model is evaluated on the hold-out test set of events and compared with the previous model. To perform a one-to-one comparison with GWSkyNet-Multi the model predictions are evaluated in one-vs-all mode, and the accuracy is calculated. While the accuracy differences for the models are small when comparing GWSkyNet-Multi to GWSkyNet-Multi II, the accuracies are all above 90%, indicating that the model remains in a high performance regime. Coupled with the fact that glitches in the updated dataset are harder to differentiate from the astrophysical events, and the model architecture is significantly simpler while giving more predictive information (splits the NS class and distinguishes between NSBH and BNS), the GWSkyNet-Multi II model is a significant update to the original model.

A comparison of the GWSkyNet-Multi II classifications to the true GWTC-3 classifications shows that

the model correctly predicts 61/75 (81%) of O3 events. GWSkyNet-Multi II over-predicts the number of NSBH and BNS events, which are high potential targets for EM follow-up. On the other hand, it does not misclassify any real astrophysical events as glitches, nor any NSBH or BNS events as BBH. This means that the model is conservative in “downgrading” the classification of an event to a less promising class for follow-up. While the overall O3 accuracy is the same as for GWSkyNet-Multi, the type of events that are misclassified are different. In particular the BNS event S190425z is correctly predicted by the new model, while it was classified as a glitch before. Analysis of the misclassifications shows that GWSkyNet-Multi II does not have the same biases that are present in the original model, and in particular does not disproportionately struggle with events involving the Virgo detector. An analysis of the model dependence on the inputs in the context of misclassifications reveals no simple linear relationship or bias, suggesting that the model has learned non-linear feature representations through the combination of the inputs to distinguish classes.

With the updated model, we also provide the GWSkyNet-Multi II predictions for select significant event alerts that have been issued during O4, up to the end of December 2024. A list of all O4 event predictions, including for the latest event alerts, is maintained by the authors and publicly available⁹. When compared to the latest updated LVK classifications for an initial analysis, GWSkyNet-Multi II correctly predicts 93% of these alerts, which is similar to the prediction accuracy of the LVK preliminary alerts (92%). While a complete comparison and analysis will be performed after the end of O4, once the LVK final catalog of events becomes available, the high accuracy of GWSkyNet-Multi II in this initial analysis illustrates the utility of the model.

Analysis of the updated model’s predictions on all the varied data sets across observing runs shows that GWSkyNet-Multi II provides more robust and informative predictions for use by the community to make follow-up observation decisions. A git repository containing the updated model, together with scripts and instructions on how to use the model, is publicly available¹⁰. In future work we plan to study the model with machine learning explainability methods to shed further light on the model’s inner workings and its learned decision boundaries. We also aim to expand the model’s capabilities in O5 and beyond to potentially classify early

⁹ <https://nayer-raza.github.io/projects/GWSkyNet-Multi/>

¹⁰ <https://github.com/nayer-raza/GWSkyNet-Multi>

warning alerts and produce estimates for the masses of the compact objects in candidate CBC alerts.

The authors wish to acknowledge and highlight the contributions of Miriam Cabero, Thomas Abbott, Eitan Buffaz, and Nicholas Vieira in developing the original version of the model, `GWSkyNet-Multi`. The authors also wish to thank members of the ML-ESTEEM collaboration, in particular Frédéric Beupré, Renée Hložek, Flavie Lavoie-Cardinal, and Niko Lecoche, for their insights and discussions that helped guide this work.

The authors acknowledge support for this project from the Canadian Tri-Agency New Frontiers in Research Fund - Exploration program, and from the Canadian Institute for Advanced Research (CIFAR), in particular the CIFAR Catalyst program in supporting the ML-ESTEEM collaboration. N.R. is supported by a Walter C. Sumner Memorial Fellowship and acknowledges funding support from the Trottier Space Institute at McGill. D.H. and J.M. acknowledge support from the Natural Sciences and Engineering Research Council of Canada (NSERC) Discovery Grant program and the Canada Research Chairs (CRC) program. A.M. acknowledges support from the NSF (1640818, AST-1815034). A.M. and J.M. also acknowledge support from IUSSTF (JC-001/2017). This material is based upon work supported by NSF’s LIGO Laboratory, which is a major facility fully funded by the National Science Foundation.

APPENDIX

A. RE-WEIGHTING NSBH AND BNS EVENTS

The training dataset has equal numbers of samples for each of the four classes, but in reality their occurrence rates are quite different. In particular, NSBH and BNS merger events are rare compared to BBH mergers and glitches: of the 90 significant CBC events reported by the LVK between O1 and O3, 83 are confidently classified as BBH events ($M_1, M_2 > 3 M_\odot$) (Abbott et al. 2019, 2024, 2023a). Similarly, of the 75 CBC candidate public alerts issued in O3, there were: 32 Glitch, 40 BBH, 2 NSBH, and 1 BNS. Providing a class-balanced dataset during training helps the model to learn the differences between the classes, but for our model this also leads to over-predicting the number of BNS and NSBH events as compared to the real number of O3 events.

We attempt to correct for this and find that down-weighting the NSBH events during training by a factor of 5 and the BNS events by a factor of 10, as compared to the BBH and glitch events, helps prevent the model from over-predicting the occurrence of these events. This has

a marginal negative impact on the model’s test set performance (which is still class balanced), but a significant positive effect on its performance on O3 public alerts, as seen in Table 5, which shows experiments performed for a range of different down-weighting values. A down-weighting of BNS by a factor of 10 and NSBH by a factor of 5 strikes the right balance: 3% loss in test accuracy, for a 16% gain in O3 accuracy. The drop in performance between the test and O3 datasets is not completely surprising, since these follow different distributions, and the gap is indicative of the differences in the training dataset (which includes simulated events) and the real merger population. We find that the down-weighting helps the model learn different decision boundaries for input features, which generalize better to actual alerts in O3. Of course these preliminary results are optimistic (over-fitted to O3) since they rely on knowing the exact distribution of classes in O3. Generalization will be evaluated on the O4 dataset once it is publicly released.

Down-weighting Factor		Model Accuracy (%)	
NSBH	BNS	Test Set	O3 Events
1	1	87.8 ± 1.5	65.3
2	2	87.9 ± 1.3	69.3
2	4	86.9 ± 1.4	69.3
5	5	85.9 ± 1.4	76.0
5	10	85.1 ± 1.3	81.3
10	10	83.5 ± 1.3	81.3
10	20	83.0 ± 1.4	81.3
20	20	80.6 ± 1.9	81.3
20	40	80.5 ± 1.9	82.7

Table 5. Experiments in down-weighting the NSBH and BNS events in the model training (as compared to the BBH and glitch events), and their impact on the model’s test set accuracy and O3 events accuracy. The drop of performance between the test and O3 datasets reflects how well the features learned by the model in the training generalize to the distribution of events in O3. A down-weighting of BNS by a factor of 10 and NSBH by a factor of 5 strikes the optimal balance: a marginal 3% loss in test accuracy, for a 16% gain in O3 accuracy.

Instead of down-weighting, we could also have a non class-balanced training set, reducing the number of NSBH and BNS events (e.g., training on 150 BNS events instead of 1500). The disadvantage of this approach is that we lose variety in the type of BNS and NSBH events that the model can learn.

B. O3 CLASSIFICATIONS ANALYSIS BASED ON INPUTS

We provide a comparison of the O3 events correctly classified and misclassified by *GWSkyNet-Multi II* in the context of the model input values in Figure 6. Aside from the 5 BBH events that are misclassified as NSBH having mean distances at the lower end of the distribution, there are no other straightforward boundary regions identified in this analysis. This suggests that the model does not have a linear dependence on any one input, but distinguishes classes from a non-linear combination of the inputs codified in the deep neural network.

REFERENCES

- Aasi, J., Abbott, B. P., Abbott, R., et al. 2015, *Classical and Quantum Gravity*, 32, 074001, doi: [10.1088/0264-9381/32/7/074001](https://doi.org/10.1088/0264-9381/32/7/074001)
- Abadi, M., Agarwal, A., Barham, P., et al. 2015, *TensorFlow: Large-Scale Machine Learning on Heterogeneous Systems*. <https://www.tensorflow.org/>
- Abbott, B. P., Abbott, R., Abbott, T. D., et al. 2017a, *PhRvL*, 119, 161101, doi: [10.1103/PhysRevLett.119.161101](https://doi.org/10.1103/PhysRevLett.119.161101)
- . 2017b, *ApJL*, 848, L12, doi: [10.3847/2041-8213/aa91c9](https://doi.org/10.3847/2041-8213/aa91c9)
- . 2017c, *ApJL*, 848, L13, doi: [10.3847/2041-8213/aa920c](https://doi.org/10.3847/2041-8213/aa920c)
- . 2017d, *Nature*, 551, 85, doi: [10.1038/nature24471](https://doi.org/10.1038/nature24471)
- . 2018, *Classical and Quantum Gravity*, 35, 065010, doi: [10.1088/1361-6382/aaaafa](https://doi.org/10.1088/1361-6382/aaaafa)
- . 2019, *Physical Review X*, 9, 031040, doi: [10.1103/PhysRevX.9.031040](https://doi.org/10.1103/PhysRevX.9.031040)
- . 2020, *Classical and Quantum Gravity*, 37, 055002, doi: [10.1088/1361-6382/ab685e](https://doi.org/10.1088/1361-6382/ab685e)
- Abbott, R., Abbott, T. D., Acernese, F., et al. 2021a, *GWTC-2.1 Candidate Data Release, v3*, Zenodo, doi: [10.5281/zenodo.5759108](https://doi.org/10.5281/zenodo.5759108)
- . 2021b, *GWTC-3 Candidate Data Release*, Zenodo, doi: [10.5281/zenodo.5546665](https://doi.org/10.5281/zenodo.5546665)
- . 2023a, *Physical Review X*, 13, 041039, doi: [10.1103/PhysRevX.13.041039](https://doi.org/10.1103/PhysRevX.13.041039)
- . 2023b, *Physical Review X*, 13, 011048, doi: [10.1103/PhysRevX.13.011048](https://doi.org/10.1103/PhysRevX.13.011048)
- . 2024, *PhRvD*, 109, 022001, doi: [10.1103/PhysRevD.109.022001](https://doi.org/10.1103/PhysRevD.109.022001)
- Abbott, T. C., Buffaz, E., Vieira, N., et al. 2022, *ApJ*, 927, 232, doi: [10.3847/1538-4357/ac5019](https://doi.org/10.3847/1538-4357/ac5019)
- Acernese, F., Agathos, M., Agatsuma, K., et al. 2015, *Classical and Quantum Gravity*, 32, 024001, doi: [10.1088/0264-9381/32/2/024001](https://doi.org/10.1088/0264-9381/32/2/024001)
- Akiba, T., Sano, S., Yanase, T., Ohta, T., & Koyama, M. 2019, in *Proceedings of the 25th ACM SIGKDD International Conference on Knowledge Discovery & Data Mining, KDD '19 (New York, NY, USA: Association for Computing Machinery)*, 2623–2631, doi: [10.1145/3292500.3330701](https://doi.org/10.1145/3292500.3330701)
- Akutsu, T., Ando, M., Arai, K., et al. 2021, *Progress of Theoretical and Experimental Physics*, 2021, 05A101, doi: [10.1093/ptep/ptaa125](https://doi.org/10.1093/ptep/ptaa125)
- Aubin, F., Brighenti, F., Chierici, R., et al. 2021, *Classical and Quantum Gravity*, 38, 095004, doi: [10.1088/1361-6382/abe913](https://doi.org/10.1088/1361-6382/abe913)
- Barbieri, C., Salafia, O. S., Perego, A., Colpi, M., & Ghirlanda, G. 2020, *European Physical Journal A*, 56, 8, doi: [10.1140/epja/s10050-019-00013-x](https://doi.org/10.1140/epja/s10050-019-00013-x)

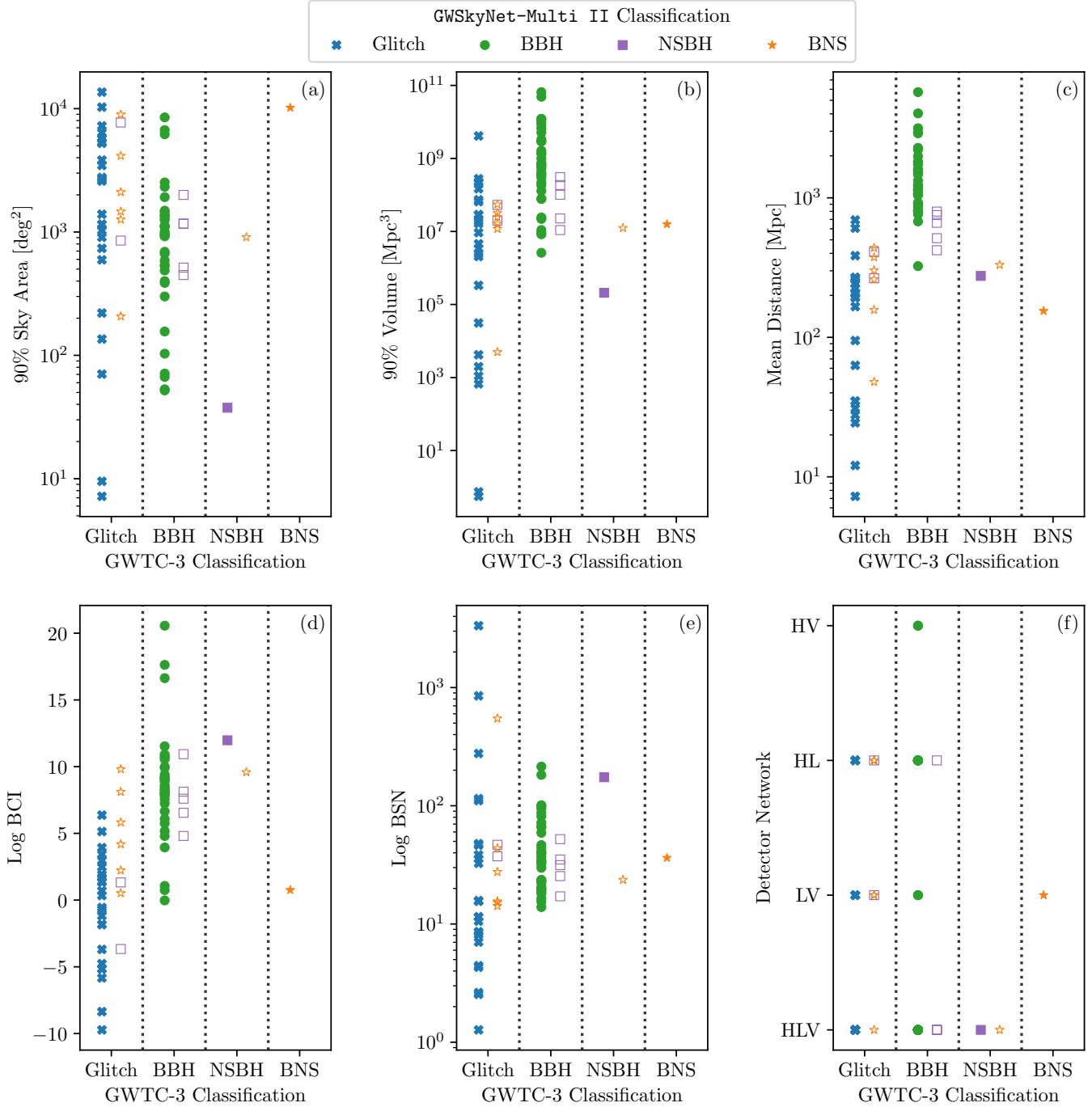


Figure 6. Classifications of the 75 multi-detector candidate CBC events in O3 for which a public alert was issued, distributed vertically by the input parameters: (a) sky map localization area, (b) 3D volume localization, (c) estimated mean distance, (d) Bayes factor for coherence vs. incoherence, (e) Bayes factor for signal vs. noise, and (f) observing detector network. In each panel the events are horizontally divided according to their true classification from GWTC-3: 32 glitch events in the left column, 40 BBH events in the center-left column, 2 NSBH events in the center-right column, and 1 BNS event in the right column. The marker for each event is labeled according to its predicted classification from **GWSkyNet-Multi II**: glitches in blue crosses, BBH in green circles, NSBH in purple squares, and BNS in orange stars. Events that are correctly classified by **GWSkyNet-Multi II** have filled markers (e.g., the filled blue crosses for glitches in the glitch column), while misclassified events have open markers that are slightly offset to the right (e.g., the unfilled orange stars for BNS in the glitch column). The misclassified events are compared to the correct classifications to find regions in the input values where the misclassifications might stand out. Aside from the 5 BBH events that are misclassified as NSBH having mean distances at the lower end of the distribution, there are no other straightforward boundary regions identified in this analysis.

- Bohé, A., Shao, L., Taracchini, A., et al. 2017, *PhRvD*, 95, 044028, doi: [10.1103/PhysRevD.95.044028](https://doi.org/10.1103/PhysRevD.95.044028)
- Branchesi, M., Stamerra, A., Salafia, O. S., Piranomonte, S., & Patricelli, B. 2021, in *Handbook of Gravitational Wave Astronomy* (Springer Singapore), 22, doi: [10.1007/978-981-15-4702-7_22-1](https://doi.org/10.1007/978-981-15-4702-7_22-1)
- Cabero, M., Mahabal, A., & McIver, J. 2020, *ApJL*, 904, L9, doi: [10.3847/2041-8213/abc5b5](https://doi.org/10.3847/2041-8213/abc5b5)
- Cannon, K., Caudill, S., Chan, C., et al. 2021, *SoftwareX*, 14, 100680, doi: [10.1016/j.softx.2021.100680](https://doi.org/10.1016/j.softx.2021.100680)
- Chan, M. L., McIver, J., Mahabal, A., et al. 2024, *ApJ*, 972, 50, doi: [10.3847/1538-4357/ad496a](https://doi.org/10.3847/1538-4357/ad496a)
- Chen, T., & Guestrin, C. 2016, in *Proceedings of the 22nd ACM SIGKDD International Conference on Knowledge Discovery and Data Mining, KDD '16* (New York, NY, USA: Association for Computing Machinery), 785–794, doi: [10.1145/2939672.2939785](https://doi.org/10.1145/2939672.2939785)
- Chollet, F., et al. 2015, *Keras*, <https://keras.io>
- Dal Canton, T., Bhagwat, S., Dhurandhar, S. V., & Lundgren, A. 2014, *Classical and Quantum Gravity*, 31, 015016, doi: [10.1088/0264-9381/31/1/015016](https://doi.org/10.1088/0264-9381/31/1/015016)
- Davies, G. S., Dent, T., Tápai, M., et al. 2020, *PhRvD*, 102, 022004, doi: [10.1103/PhysRevD.102.022004](https://doi.org/10.1103/PhysRevD.102.022004)
- Drozda, P., Belczynski, K., O’Shaughnessy, R., Bulik, T., & Fryer, C. L. 2022, *A&A*, 667, A126, doi: [10.1051/0004-6361/202039418](https://doi.org/10.1051/0004-6361/202039418)
- Ghonge, S., Brandt, J., Sullivan, J. M., et al. 2024, *PhRvD*, 110, 122002, doi: [10.1103/PhysRevD.110.122002](https://doi.org/10.1103/PhysRevD.110.122002)
- Hourihane, S., Chatziioannou, K., Wijngaarden, M., et al. 2022, *PhRvD*, 106, 042006, doi: [10.1103/PhysRevD.106.042006](https://doi.org/10.1103/PhysRevD.106.042006)
- Kingma, D. P., & Ba, J. 2014, *arXiv e-prints*, arXiv:1412.6980, doi: [10.48550/arXiv.1412.6980](https://doi.org/10.48550/arXiv.1412.6980)
- Landry, P., & Read, J. S. 2021, *ApJL*, 921, L25, doi: [10.3847/2041-8213/ac2f3e](https://doi.org/10.3847/2041-8213/ac2f3e)
- Ligo Scientific Collaboration, VIRGO Collaboration, & Kagra Collaboration. 2024, *GRB Coordinates Network*, 36812, 1
- Lou, Y., Caruana, R., Gehrke, J., & Hooker, G. 2013, in *Proceedings of the 19th ACM SIGKDD International Conference on Knowledge Discovery and Data Mining, KDD '13* (New York, NY, USA: Association for Computing Machinery), 623–631, doi: [10.1145/2487575.2487579](https://doi.org/10.1145/2487575.2487579)
- Macas, R., Pooley, J., Nuttall, L. K., et al. 2022, *PhRvD*, 105, 103021, doi: [10.1103/PhysRevD.105.103021](https://doi.org/10.1103/PhysRevD.105.103021)
- Metzger, B. D. 2019, *Living Reviews in Relativity*, 23, 1, doi: [10.1007/s41114-019-0024-0](https://doi.org/10.1007/s41114-019-0024-0)
- Mishra, C. K., Kela, A., Arun, K. G., & Faye, G. 2016, *PhRvD*, 93, 084054, doi: [10.1103/PhysRevD.93.084054](https://doi.org/10.1103/PhysRevD.93.084054)
- Nori, H., Jenkins, S., Koch, P., & Caruana, R. 2019, *arXiv e-prints*, arXiv:1909.09223, doi: [10.48550/arXiv.1909.09223](https://doi.org/10.48550/arXiv.1909.09223)
- Pankow, C., Chatziioannou, K., Chase, E. A., et al. 2018, *PhRvD*, 98, 084016, doi: [10.1103/PhysRevD.98.084016](https://doi.org/10.1103/PhysRevD.98.084016)
- Payne, E., Hourihane, S., Golomb, J., et al. 2022, *PhRvD*, 106, 104017, doi: [10.1103/PhysRevD.106.104017](https://doi.org/10.1103/PhysRevD.106.104017)
- Powell, J. 2018, *Classical and Quantum Gravity*, 35, 155017, doi: [10.1088/1361-6382/aacf18](https://doi.org/10.1088/1361-6382/aacf18)
- Raza, N., Chan, M. L., Haggard, D., et al. 2024, *ApJ*, 963, 98, doi: [10.3847/1538-4357/ad13ea](https://doi.org/10.3847/1538-4357/ad13ea)
- Singer, L. P., & Price, L. R. 2016, *PhRvD*, 93, 024013, doi: [10.1103/PhysRevD.93.024013](https://doi.org/10.1103/PhysRevD.93.024013)
- Udall, R., Hourihane, S., Miller, S., et al. 2024, *arXiv e-prints*, arXiv:2409.03912, doi: [10.48550/arXiv.2409.03912](https://doi.org/10.48550/arXiv.2409.03912)
- Vieira, N., Ruan, J. J., Haggard, D., et al. 2020, *ApJ*, 895, 96, doi: [10.3847/1538-4357/ab917d](https://doi.org/10.3847/1538-4357/ab917d)